31st Annual International Conference of the IEEE EMBS
Minneapolis, Minnesota, USA, September 2-6, 2009

Improved Separability Of Dipole Sources By Tripolar Versus Conventional Disk Electrodes: A Modeling Study Using Independent Component Analysis

H. Cao, W. Besio, S. Jones, and A. Medvedev

Abstract—**Tripolar electrodes have been shown to have less mutual information and higher spatial resolution than disc electrodes. In this work, a four-layer anisotropic concentric spherical head computer model was programmed, then four configurations of time-varying dipole signals were used to generate the scalp surface signals that would be obtained with tripolar and disc electrodes, and four important EEG artifacts were tested: eye blinking, cheek movements, jaw movements, and talking. Finally, a fast fixed-point algorithm was used for signal independent component analysis (ICA). The results show that signals from tripolar electrodes generated better ICA separation results than from disc electrodes for EEG signals with these four types of artifacts.**

I. INTRODUCTION

Independent component analysis (ICA) is a computational method for separating a multivariate signal into additive subcomponents assuming there is mutual statistical independence of the non-Gaussian source signals [1]. To the best of our knowledge, ICA was first applied to encephalography (EEG) by Makeig et al. (1996) and is now widely accepted in the EEG research community; most often to detect and remove stereotyped eye, muscle, and line noise artifacts [2][3]. Ventoura et al. used ICA for reconstructing averaged event-related potentials (ERPs) in the time window of the P600 component, selecting a subset of independent components' projections to the original electrode recording positions [4]. Basically Ventoura et al. used ICA as a filter.

However, ICA also has been used to separate biologically plausible brain sources whose activity patterns are distinctly linked to behavioral phenomena [5]. Many of the biologically plausible sources ICA identifies in EEG data have scalp maps nearly fitting the projection of a single equivalent current dipole [6,7] and are therefore compatible with the projection to the scalp electrodes of synchronous local field activity within a connected patch of cortex.

Fast ICA is an efficient and popular algorithm invented by Aapo Hyvärinen at Helsinki University of Technology [8]. The algorithm has cubic convergence speed and does not require parameter adjustment.

Concentric electrodes outperform disc electrodes with higher signal-to-noise ratio (SNR), higher spatial selectivity, and lower mutual information (MI), which should be beneficial for the field of EEG [9]-[11]. Further, McFarland et al. concluded that the common average and the Laplacian derivation yield good performance on EEG classification [12]. Babiloni et al. demonstrated that the surface Laplacian transformation of EEG signals can improve the recognition scores of imagined motor activity [13] [14].

Munck et al. [15], to our knowledge, were among the first to use the four-layer anisotropic concentric spherical head model, with Zhou and van Oosterom revising its numerical computation method [16]. In this work, a fast algorithm was developed for the four-layer anisotropic concentric spherical head model, calculating the potentials hundreds of times faster than the Zhou - van Oosterom algorithm. Also, a coordinate translation algorithm was implemented so that potentials at any scalp surface location from multiple dipoles with arbitrary moment vectors at any given positions within the head could be calculated.

Sine wave, rectangular, rising cosine and white noise signals, were used for the dipole sources of our four concentric spheres model. Four important EEG artifacts were tested: eye blinking, cheek movements, jaw movements, and talking. Different numbers and size of the electrodes for both tripolar electrodes and disc electrodes were used in simulating the surface potentials. The ICA results showed that, in this work, the modeled signals from tripolar electrodes gave better ICA separation results than from disc electrodes.

II. METHOD

A. Four-layer head model and its fast numerical calculation algorithm

Equation (1) is used to calculate the dipole generated potential at the scalp surface in the four-layer head model [15].

H. Cao, was with Tianjin University, Tianjin, China. He is now with the Department of Biomedical Engineering, Louisiana Tech University, LA 71270 USA (e-mail: hca009@latech.edu).

W. Besio is a IEEE senior member and is in the Electrical, Computer, and Biomedical Engineering Department at the University of Rhode Island, Kingston, RI 02881 USA. (e-mail: besio@ele.uri.edu).

S. Jones is with the Department of Biomedical Engineering, Louisiana Tech University, LA 71270 USA (email: sajones@coes.latech.edu).

A. Medvedev is with the Department of Neurology, Georgetown University, Washington, DC, USA. Washington, DC, USA. (email: am236@georgetown.edu).

$$\psi_{dip} = \frac{1}{4\pi}\sum_{n=1}^{\infty}\frac{R_n^{(2)}(r)}{\varepsilon_4 B_4^{(2)}}\{M_r R_n^{(1)}(r_0)P_n^0(\cos\theta) + M_\theta r_0^{-1} R_n^1(r_0)P_n^0(\cos\theta)\cos\phi\} \quad (1)$$

where P_n^0 and P_n^1 are the associated Legendre functions, and M_θ and M_r are the radial and tangential component of the dipole vector, respectively. Please see [15] for the other notations involved in the above formula. Numerical calculation [16] of the four layer head model was improved in two aspect:

1. Calculation speed improvement using database method;
2. Generalization of the dipole source positions and dipole moment vectors using coordinate translation.

B. Independent Component analysis and its Fast Fixed-Point Algorithm

The basic steps for calculating ICA are shown below:

$$PC = \text{PRINCOMP}(v) \quad (2)$$

$$y = PC^T v \quad (3)$$

$$D = 1/\sqrt{\text{cov}(y)} \quad (4)$$

$$x = D\,y \quad (5)$$

$$\text{S} = \text{B}^{\text{T}}\text{x} \quad (6)$$

Where $v = [v_1, v_2, ..., v_n]'$ are the zero-mean signals acquired by electrodes, in our case calculated at the electrode locations; PC is the orthonormal transformation matrix of v, which was calculated with Matlab, and has the unit variance for each column; y is the projected vector; D is a transfer matrix; the mean of x is not necessarily zero, but $E\{x\,x^T\} = I$. B is the orthogonal matrix ($BB^T = I$) to be found by the fast fixed-point ICA method [8]. S is the ICA separation results – the separate sources.

C. *Source dipoles distribution and wave forms*

Sine wave, rectangular, rising cosine and white noise signals, were used for the dipole sources (Fig. 3-4, first row of waves). The dipoles can be set at any locations within the head.

D. EEG artifact simulation

To perform a comparison under controlled conditions four artifacts [17]: eye blinking, cheek movements, jaw movements, and talking were recorded and combined with the simulated signals at the electrodes. The SNR was calculated by determining the signal and noise power in the frequency domain for the recorded signals from tripolar and disc electrodes respectively and were:

snr_t=[13,18,23,28]; (7)

snr_d=[-28,-17,-13,-7]; (8)

Where the snr_t and snr_d are the SNR of the tripolar and disc electrodes respectively. The amplitude of the artifact waves were simulated for each electrode with the same SNR as was determined in the recorded noise signals (Fig. 1) by [17].

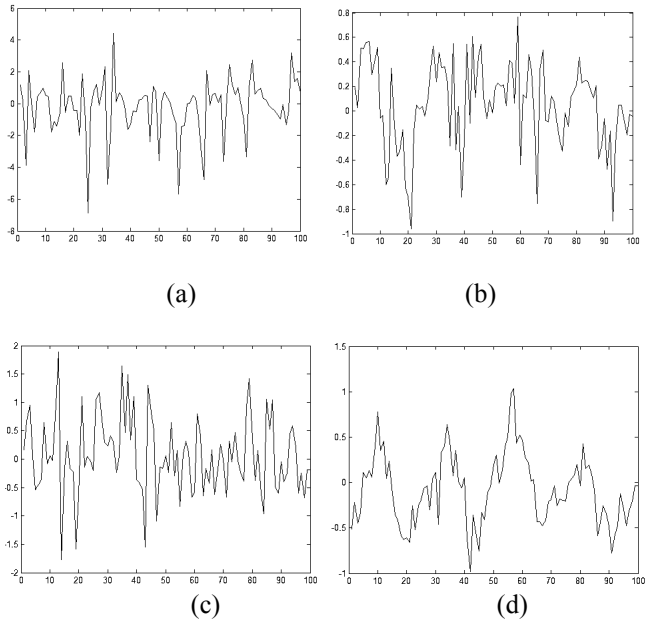

Fig. 1 Artifact waveforms of (a) eye blinking, (b) cheek movements, (c) jaw movements, and (d) talking

E. *Electrodes distribution and number of electrodes*

For the model, the electrodes can be at any position on the surface of the scalp, and the number of electrodes should not be less than the number of sources. In real conditions when the number of electrodes is given, the number of sources to be found by ICA would be less than the number of electrodes. The four electrodes in the model were placed at C3, C4, Cz, T3, though T4 and more positions were tested, using from 4 to 10 electrodes. Electrodes for the artifacts recorded by [17], and used in our model, were from C3, C4, and Cz.

III. RESULTS

A. *Higher spatial sensitivity of tripolar electrodes*

Fig. 2 shows the potentials produced by a vertically oriented unit dipole located at [58,0,0] (spherical coordinates: [radius, azimuth, zenith]; radius is in mm). Those potentials are simulated as if being recorded by a disc and a tripolar electrode located at the surface of the sphere at different angular positions from phi = 0 ("north pole" of the sphere, [75,0,0]) to phi = π ("south pole", [75,0, π]).

B. ICA results

ICA was executed with 4 to 10 electrodes. Fig. 3 are the ICA results for 10 electrodes with talking artifacts, the same

condition as in Fig.4 e1 and e2. Fig. 4 shows the wave forms of the dipoles (row a), the ICA results of signals from tripolar electrodes (row x1), and the ICA results of the signal from disc electrodes (row x2), where x is from b to e, with respect to the electrode potentials with four artifacts: (b) eye blinking, (c) cheek movements, (d) jaw movements, and (e) talking. Table 1 gives the normalized covariance for the ICA separation results and the source signals.

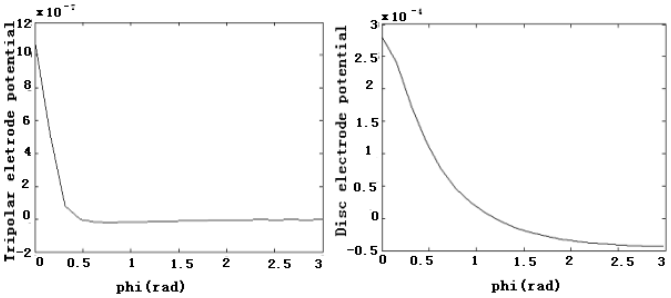

(a) (b)

Fig. 2 Calculated signals from (a) tripolar and (b) disc electrodes with no added noise.

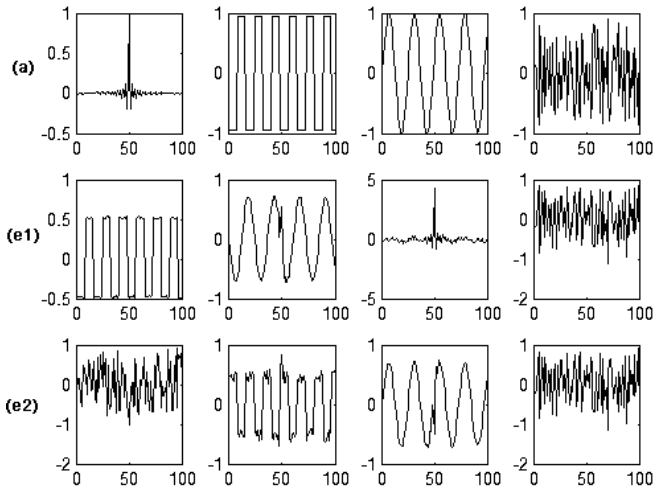

Fig. 3 ICA Separation results using 10 electrodes with talking artifacts (a) dipole source waves; (x1) Tripolar electrode ICA results ; (x2) Disc electrode ICA results

Table 1 The normalized covariance of the ICA separation results and the source signals

Cov \ Dipole source		Rising cos	Rect	Sine	White noise
Eye blink	Tripolar	0.636	0.996	0.985	0.976
	Disc	0.231	0.993	0.966	0.962
Cheek move	Tripolar	0.846	0.998	0.987	0.973
	Disc	0.231	0.985	0.980	0.972
Jaw move	Tripolar	0.942	0.999	0.997	0.974
	Disc	0.237	0.989	0.977	0.960
talk	Tripolar	0.966	0.999	0.992	0.942
	Disc	0.393	0.993	0.985	0.907

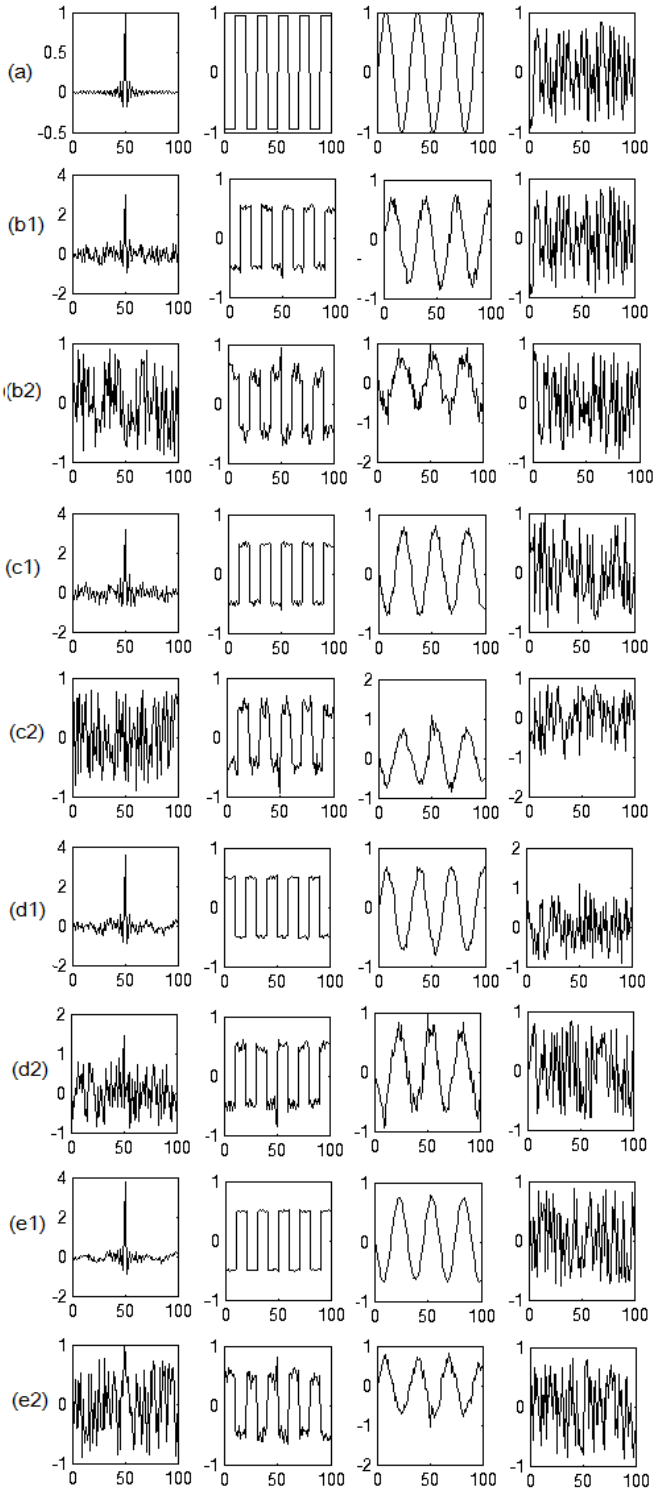

Fig. 4 ICA results from electrodes potentials with four artifacts (a) dipole source waves; (x1) ICA results from the tripolar electrode signals; (x2) ICA results from the disc electrode signals. x is from b to e, with respect to the four artifacts: (b) eye blinking, (c) cheek movements, (d) jaw movements, and (e) talking. (Vertical axis – arbitrary units, horizontal axis – time in ms.)

IV. Discussion

ICA is mainly used to separate linearly combined signals, acting as a filter. For a combined signal P which is acquired from an electrode, P can be expressed by

$$p = a_1 s_1 + a_2 s_2 + \ldots \quad (9)$$

where s_i are the uncorrelated, zero-mean, unit variance signals. Thus the weighted coefficients a_i are the amplitudes of the source signals. The greater the difference between a_i, the better the results of ICA filtering (separating). Because tripolar electrodes have high SNR, the amplitude of their signals will be relatively higher. Since they have higher spatial resolution as seen from Fig. 2 and lower mutual information, they will give greater difference of coefficients a_i for each electrode, leading to better ICA filtering. In Fig. 4, under the same conditions, the ICA results of the tripolar electrode signals extracted all the independent components with high similarity (see table 1), while the ICA results of the disc electrodes caused inaccuracy in each independent component extracted. In particular, a rising cosine component is not recognizable in the results from the disc electrodes (Fig 4 b2-e2 1st column). The higher fidelity of the tripolar electrodes may also be caused by their high rejection of common mode noise, which can be seen from the tripolar potential calculation formula [18]:

$$P_L = 16(P_{Middle} - P_c) - (P_{Outer} - P_c) \quad (10)$$

where P_{Middle}, P_{Outer} and P_c are potentials from the middle ring, the outer ring and the center disc, respectively. Since those three electrode elements are close to each other, they have nearly the same common mode noise, which becomes sharply attenuated when equation (10) is used in estimation of the Laplacian tripolar potential PL. When we consider sources such as the AC wall mains, which are generally distant from the electrodes compared to the signal source in the brain, the common mode noise rejection of the trpolar concentric electrode is beneficial.

We also found that adding more electrodes than there are sources did not improve the ICA separation of the signal sources. In Fig. 3 ten electrodes were utilized in the ICA process and there is no evident difference between Fig. 4 e1 and e2 when only 4 electrodes were utilized.

V. Summary/Conclusion

For the four EEG artifacts tested in this work, tripolar electrodes generate the best ICA separation results compared with disc electrodes. This is most likely due to the tripolar electrodes higher sensitivity to the source spatial distribution, and thus higher noise attenuation for the noise sources far from the electrode positions (head surface). Also, the tripolar electrodes' higher spatial resolution should enable them to provide more uncorrelated signals benefiting the ICA.

Acknowledgment

We would like to thank Apoorva Kakkeri for allowing us to use his data in preparation of this work.

References

[1] James V. Stone, Encyclopedia of Statistics in Behavioral Science, Volume 2, pp. 907–912, B. Everitt editor, Wiley Interscience, 2005.

[2] T.P. Jung, S. Makeig, M. Westerfield, J. Townsend, E. Courchesne T.J. Sejnowski, "Analyzing and visualizing single-trial event-related potentials," Adv Neural Inf Process Syst, vol. 11, pp. 118–24, 1999.

[3] TP. Jung, Makeig S, Humphries C, Lee TW, McKeown MJ, Iragui V, Sejnowski TJ. "Removing electroencephalographic artifacts by blind source separation," Psychophysiology, vol. 37, pp.163–168, 2000.

[4] E. Ventouras, M. Moatsos, C. Papageorgiou, A. Rabavilas, N. Uzunoglu, "Independent Component Analysis applied to the P600 component of Event-Related," Potentials Proceedings of the 26th Annual International Conference of the IEEE EMBS San Francisco, CA, USA, September 1-5, 2004.

[5] A. Delorme, S. Makeig, "EEGLAB: an open source toolbox for analysis of single-trial EEG dynamics including independent component analysis," J. Neurosci. Meth., vol. 134, pp. 9-21.

[6] T.P. Jung, S. Makeig, M. Westerfield, J. Townsend, E. Courchesne, T.J. Sejnowski, "Analysis and visualization of single-trial event-related potentials," Hum Brain Mapp, vol.14, pp. 166–185, 2001.

[7] S. Makeig, S. Westerfield, T.P. Jung, S. Enghoff, J. Townsend, E. Courchesne, T.J. Sejnowski, "Dynamic brain sources of visual evoked responses.Science," vol.295, pp:690–694, 2002.

[8] A. Hyvarinen and E. Oja, "A Fast Fixed-Point Algorithm for Independent Component analysis," Neural computation, vol. 9, pp. 1483-1492, 1997.

[9] B. He, "Brain electrical source imaging: scalp Laplacian mapping and cortical imaging," Crit Rev Biomed Eng, vol. 27, pp. 149–88, 1999.

[10] D. Farina, C. Cescon. "Concentric-ring electrode systems for noninvasive detection of single motor unit activity," IEEE Trans Biomed Eng, vol. 48, no. 11, pp. 1326–1334, 2001.

[11] K. Koka, W. G. Besio, "Improvement of spatial selectivity and decrease of mutual information of tri-polar concentric ring electrodes," J Neurosci Methods 165, 216–222, 2007.

[12] D. J. McFarland, L. M. McCane, S. V. David and J. R. Wolpaw, "Spatial filter selection for EEG-based communication," Electroenceph. Clin. Neurophysiol, vol. 103, pp. 386–394, 1997.

[13] F. Babiloni, F. Cincotti, L. Lazzarini, J. Millán, J. Mouriño, M. Varsta, J. Heikkonen, L. Bianchi, and M.G. Marciani, "Linear Classification of Low-Resolution EEG Patterns Produced by Imagined Hand Movements," IEEE Trans. Rehab. Eng., Vol. 8, No. 2, pp.186-188, June 2000.

[14] Besio W., Cao H., Zhou. P, "Application of Tripolar Concentric Electrodes and Pre-Feature Selection Algorithm for Brain-Computer Interface," IEEE Trans Neural Systems & Rehab Eng, 16(2) 191-194, 2008.

[15] J.C. De Munck, "The potential distribution in a layered anisotropic spheroidal volume conductor," J. Appl. Phys., vol. 64, pp. 464-470, 1988.

[16] Hong Zhou, Adrian van Oosterom, "Computation of the potential distribution in a four-layer anisotropic concentric spherical volume conductor," IEEE transactions on biomedical engineering, vol. 39, no. 2, pp. 154-158, Feb. 1992.

[17] A. Kakkeri, "Superior Artifact Rejection in Electroencephalography by Tripolar Electrodes in Comparison to Other Concentric Ring Electrodes," M.S. thesis, Louisiana Tech University, 2005.

[18] W. Besio, K. Koka, R. Aakula, W. Dai, "Tri-polar Concentric Ring Electrode Development for Laplacian Electroencephalography," IEEE Trans BME, Vol. 53, No. 5, pp. 926-933, 2006,.